NASA TM X-67829

CASE FILE
COPY

THE POTENTIAL OF NUCLEAR MHD ELECTRIC POWER SYSTEMS

by G. R. Seikel and L. D. Nichols
Lewis Research Center
Cleveland, Ohio

THE POTENTIAL OF NUCLEAR MHD ELECTRIC POWER SYSTEMS

G. R. Seikel and L. D. Nichols
National Aeronautics and Space Administration
Lewis Research Center

Abstract

MHD generators are uniquely capable of fully exploiting advances in high-temperature reactor technology for electric power generation. Extension of NERVA technology could make 2500 K long-life inert-gas-cooled reactors feasible. Such reactors and MHD generators mate into attractive multi-MW electric power systems for either space or ground applications. A turbo-MHD system using a turbine driven compressor is the most attractive cycle. It has high cycle efficiency and low radiator area and temperature for space applications. A space-power system with 10 MW electric output, shielded for manned missions, could achieve specific masses of 3.5 to 5 kg/kW$_e$. A ground-power station with 60 percent efficiency also appears feasible.

Introduction

The NERVA program has resulted in major advances in the technology of high temperature reactors. As discussed by Holman and Way,[1] long-life inert-gas-cooled reactors with 2500 K outlet temperatures may be on the horizon of feasibility. The high temperature capability of MHD systems gives them an inherent advantage over turbo-electric power systems in exploiting this high-temperature reactor technology.

MHD generators are potentially efficient only at multi-MW power levels. Shielded reactor specific masses, also, improve with higher power level. Thus, MHD generators and nuclear reactors naturally mate into attractive multi-MW electric power systems. These nuclear-MHD systems would be attractive both for manned-electric-propulsion missions and for terrestrial applications.

Various thermodynamic cycles can be considered for MHD power systems. In the authors' opinion, the most attractive cycle is the combined turbo-MHD cycle (Fig. 1). A schematic of the components of this cycle is shown in Fig. 2. This cycle is similar to that considered recently by Bohn et al[2] and Millionschikov[3] for nuclear-MHD ground-power stations.

The proposed turbo-MHD cycle uses recuperators, an inner-cooled compressor, and turbine reheat to improve the cycle efficiency. The turbine output is used to drive the compressors. A Brayton cycle with only an MHD generator, such as was considered in Ref. 1, would require an electric motor to drive the compressor. For typical cycle conditions the motor power would be approximately three times the net electrical power.

The analysis of Ref. 4 indicates this turbo-MHD cycle has high efficiency for both space and ground applications. This cycle, in addition, makes use of conventional turbine technology and minimizes the required temperature and pressure ratios in the MHD generator expansion. For minimum radiator-area space systems this turbo-MHD cycle

also has relatively low radiator area and temperature.

This study reviews the performance of the turbo-MHD cycle and compares it with the equivalent Brayton-MHD and Brayton-turbo-electric cycles. For the MHD cycles, a top temperature of 2500 K is assumed and two working fluids are considered: cesium seeded neon and xenon seeded neon. The cesium seed gives the best possible electrical conductivity, whereas, the xenon seed gives a completely inert working fluid. For the cycles with turbines, two turbine-inlet temperatures are considered: 1500 and 1250 K.

The cycle temperatures, efficiencies, and specific radiator areas are compared for these various space-power systems. The efficiency of the turbo-MHD system is also presented for ground-power plants.

The specific masses of man-shielded 10 MW electric space-power systems are estimated. A brief discussion is then presented of the technology of the two most critical components of such an MHD system: the reactor and the MHD generator-magnet system. Included in this discussion is a possible modification of the turbo-MHD cycle to minimize the problems associated with alkali-metal-seeded generators and reactor fission product release.

Turbo-MHD Cycle

In the turbo-MHD cycle proposed herein (Fig. 1 and 2) the working fluid is heated in a reactor to a top temperature T_{MAX}. The fluid then adiabatically expands through an MHD generator which extracts the useful electric power. The fluid then flows through the hot sides of the turbine reheater and high temperature recuperator, enters the first turbine at a temperature T_{TURB}, is expanded, reheated to T_{TURB}, expanded through the second turbine, and flows through the hot side of the low temperature recuperator. The fluid is then cooled (in the primary cooler) down to the compressor inlet temperature T_{COMP}. The flow is compressed in three intercooled stages and is then preheated before entering the reactor in the cold sides of the low and high temperature recuperators. In the analysis of this cycle the fluid flow through all components except the generator, turbine, and compressor occur at nearly constant pressure (see Fig. 1). Friction losses are accounted for by assuming that the fractional pressure drops, $(\delta = \Delta p/p)$ are equal in the six nearly constant pressure processes shown in Fig. 1.

The MHD generator efficiency, η_{GEN}, is defined as the ratio of the electric power output, P_e, to the power that would be produced in an isentropic expansion through the generator expansion ratio, $1/(1-\delta)r_{GEN}$. The turbine efficiency, η_{TURB}, and expansion ratio, $1/(1-\delta)r_{TURB}$, are assumed equal for both turbines. The overall cycle compression ratio, r, is defined as the ratio of the compressor outlet pressure, P_H, to the turbine outlet pressure, P_L. Each of the three compressors is assumed to have the

TM X-67829

same inlet temperature, compression ratio, and efficiency (η_{COMP}). The compressors consume the total power output of the turbines. For both the reheater and the high temperature recuperator, a fraction of the total thermal power being transfered is assumed lost. The low temperature recuperator has an effectiveness of η_r. In most practical systems, all the coolers in the cycle would most likely be gas to liquid heat exchangers. However, for simplicity, no temperature drop has been accounted for between the gas working fluid and a final heat sink (for space systems the radiator). The assumed values for the performance of the cycle components are summarized in Table 1.

Cycle Efficiency

Following the analysis of Nichols,[4] the overall cycle efficiency, η, of the turbo-MHD cycle is given by

$$\eta = \frac{G}{0.05 + 0.95\,G + \frac{T_{TURB}}{T_{MAX}}\left[B(1+\eta_r) - \eta_r + 0.95\right] - \frac{T_{COMP}}{T_{MAX}}(1+C)(1-\eta_r)} \tag{1}$$

where G, B, and C are dimensionless parameters proportional to the generator, turbine, and compressor power respectively and are given by the following:

$$G = \eta_{GEN}\left\{1 - \left[r_{GEN}(1-\delta)\right]^{-\frac{\gamma-1}{\gamma}}\right\} \tag{2}$$

$$B = \eta_{TURB}\left\{1 - \left[r_{TURB}(1-\delta)\right]^{-\frac{\gamma-1}{\gamma}}\right\} \tag{3}$$

$$C = \frac{1}{\eta_{COMP}}\left[\left(\frac{r^{1/3}}{1-\delta}\right)^{\frac{\gamma-1}{\gamma}} - 1\right] \tag{4}$$

The condition that the turbine power equals the compressor power gives

$$2BT_{TURB} = 3CT_{COMP} \tag{5}$$

The overall cycle compression ratio, r, is

$$r = r_{GEN}\,r_{TURB}^2 \tag{6}$$

Ground Power Station

For a turbo-MHD ground-power station, the compressor-inlet temperature, T_{COMP}, is assumed to be equal to the available heat-sink temperature. For the cycle evaluated herein, a heat-sink temperature of 300 K is assumed. This would correspond to the temperature of ambient cooling water. An air cooled convector radiator could also be used as a heat sink; however, its temperature would be somewhat higher.

For the assumed compressor-inlet temperature, the generator and the turbine expansion ratios can then be evaluated from Eqs. (5) and (6) using Eqs. (3) and (4). Substitution of these compression ratios into Eq. (1) using Eqs. (2) through (4) yields the efficiency of the ground-power station.

For a given temperature reactor and turbine, the cycle efficiency is a function of the MHD generator efficiency, the cycle compression ratio, and the fractional pressure drop, δ.

The parametric variation of the cycle efficiencies of turbo-MHD ground power stations having reactor temperatures of 2500 K and turbine temperatures of either 1500 or 1250 K are shown in Figure 3. It indicates how the efficiency varies with each of the cycle parameters. The efficiency is the most sensitive to the generator efficiency and the recuperator effectiveness. The crossing of the two turbine temperature curves as a function of η_r results from the fact that for each recuperator effectiveness there is an optimum turbine temperature. Figure 3 shows that an overall cycle efficiency of above 60 percent should be obtainable with a 2500 K turbo-MHD ground-power station.

Space Power System

For a space-power system the compressor-inlet temperature is adjusted to obtain the optimum specific radiator area (radiator area, A_{RAD}, divided by the output electric power, P_e). For simplicity, the generator and turbine expansion ratios are assumed equal. The specific radiator area can be expressed as

$$\frac{A_{RAD}}{P_e} = \frac{\alpha}{\epsilon\sigma T_{MAX}^4} \tag{7}$$

Where ϵ is the radiator emissivity (assumed 0.9), σ is the Stephen Boltzman constant, and α is a dimensionless parameter relating the effective-radiator and reactor temperatures with the power output. This parameter may be written as:

$$\alpha = \frac{1}{G}\left(\frac{T_{MAX}}{T_{TURB}}\right)^3\left(\frac{3C}{2B}\right)^3\left(1 + \frac{1}{3(1+C)^3}\left\{2 + \left[\eta_r + (1-\eta_r)\frac{3}{2}\frac{C}{B}\frac{(1-B)}{(1+C)}\right]^{-3}\right\}\right) \tag{8}$$

assuming that the radiator is radiating to absolute zero and there is no temperature difference between the radiator and the working fluid in the coolers.

Using Eqs. (7) and (8) and Eqs. (1) through (5), leads to setting a compression ratio (hence also a compressor-inlet temperature) which minimizes the specific radiator area. This minimum value of specific radiator area decreases with decreasing fractional pressure drop, δ. However, the low-temperature recuperator specific area increases with decreasing fractional pressure drop (because of reduced heat transfer). The specific area of the low temperature recuperator is

$$\frac{A_r}{P_e} = \frac{(\gamma-1)}{\gamma}\frac{8\sqrt{2}}{P_H}\frac{N_{PR}}{\sqrt{RT_{MAX}}}\frac{\mathscr{R}}{f} \tag{9}$$

where $\mathscr{R}$ depends upon the same parameters as α and is given by:

$$\mathcal{R} = \sqrt{\frac{T_{TURB}}{T_{MAX}}} \; \frac{\sqrt{\frac{1-B}{2} + \frac{B(1+C)}{3C}}}{\sqrt{\delta G \left(1 + \frac{1}{r}\right)}} \cdot \left(\frac{\eta_r}{1 - \eta_r}\right)^{3/2} \quad (10)$$

and the values of the other quantities in Eq. (9) used herein are given in Table 2.

If a value of specific recuperator area is chosen, Eq. (9) fixes the specific recuperator parameter $\mathcal{R}$. Then Eq. (10) provides a relationship between the overall compression ratio, r, and the fractional pressure drop, δ. Using this relationship in Eq. (8), one obtains the r and δ values which minimize α.

Figure 4 shows the specific radiator area as a function of cycle efficiency for space power systems having a specific recuperator area of 0.374 m^2/kW_e, turbine-inlet temperatures of 1250 or 1500 K, and MHD generator efficiencies of 80 percent (cesium seed) or 55 percent (xenon seed). These are considered to be the reasonable upper limits achievable for these two seed materials. The characteristics and technology of the generator are discussed in more detail in a later section of this paper. Also shown in Fig. 4 are the equivalent curves for all-MHD cycles with cesium and xenon seeds, i.e. cycles in which the compressor is driven by an electric motor which is powered by part of the output of the MHD generator. Also shown in the figure is a curve for a turbo-electric power system with a reactor-outlet temperature of 1500 K. A 1250 K turbo-electric system was also considered, but it is off the scale of Fig. 4.

A summary of the cycle parameters for that system and the other power systems shown in Fig. 4 for the minimum specific radiator area points is given in Table 3. Table 3 shows that the most attractive features of the turbo-MHD space-power system are (1) the high cycle efficiency, (2) the relatively low radiator area, (3) the relatively low radiator temperature compared to the high performance all-MHD system, (4) the low ratio of compressor power to net electrical power, (5) the relatively low temperature and pressure ratios required in the MHD generator expansion, and (6) the lower sensitivity of the cycle performance to the MHD generator seed than the all-MHD system.

Mass Estimates

Reactor Plus Shield

To estimate the mass of the reactor plus shield of a ten megawatt man shielded system the approximate method presented by Moeckel[5] was used. A cylindrical reactor having an L/D of one and a thermal power density of 100 W/cm^3 was assumed. The two shield configurations shown in Fig. 5 were considered. The first is a 10° included angle shadow shield. The second configuration is a shadow plus peripheral shield. Both shield configurations use an inner tungsten shield to reduce the dose from gamma radiation and an outer lithium hydride shield to attenuate the neutron dose. To make the mass estimates a total dose rate of 10^{-2} rem/hr is assumed at the surface of the shadow shields and a dose rate of 1 rem/hr is assumed at the surface of the peripheral shield. Additional attenuation of these dose rates would occur in practical systems due to both distance and any cabin shielding.

Using the above assumptions and the approximate method of Moeckel one obtains the results shown in Fig. 6 for the specific mass of the reactor plus shield as a function of reactor thermal power level. For comparison purposes, also shown in Fig. 6 are a number of specific masses calculated for more detailed man-shielded reactor studies.[6,7,8,9] The open symbols are for shadow shielded reactors and the solid symbols are for reactors designed with both a shadow and a peripheral shield. As indicated in the figure, the approximate method of Moeckel appears to give quite adequate estimates of the reactor plus shield specific mass. This study will use both curves of this figure for estimating reactor plus shield mass.

Radiator

The radiator mass is estimated on the basis of a 8.4 kg/m^2 specific mass. This value was calculated by Haller and Lieblein[10] for a vapor-chamber fin-tube radiator for a Rankine power system with a 37.6 m^2 radiating area at 945 K. Their radiator makes use of segmented vapor-chamber fins but the tubes and headers are not segmented. The radiator mass breakdown is 18 percent headers, 53 percent tubes, and 29 percent fins.

Analyses such as Ref. 10 would yield substantially higher specific masses for the large ($\sim 10^3$ m^2) radiators required herein. This results primarily from the increased armor thickness required for the larger radiators to obtain the same tube and header nonpuncture probability for meteoroid impact. In the authors opinion, to accept such a specific mass penalty for large radiators is not realistic. If the vapor-chamber fin segments of a large radiator were constructed identically to those of Ref. 10, then the probable percent surviving (i.e. not penetrated by meteorites) would not vary with radiator size and the probable statistical deviation would decrease for larger radiators. By also segmenting the tubes and headers of a large radiator, their percent contribution to the radiator mass should easily be maintained at the 71 percent calculated for the smaller radiator of Ref. 10. Johnsen[11] indicates how segmenting the tubes of a tube-fin radiator lowers its mass. The authors opinion is therefore that the radiator specific mass (8.4 kg/kW) assumed for this study may be pessimistic since it is based on a radiator with good fin design but with tubes and headers that may be heavier than required. The radiators required herein, also, may be lighter because of their lower temperature.

Other Components

The other components considered in making a system mass estimate are the low-temperature recuperator, the magnet plus MHD generator, and the turbine-compressor. The masses of the high-temperature recuperator and the reheater are not considered because they have a large ΔT between the hot and cold sides of the heat exchanger (>300 K), they should, thus, be much lighter than the low-temperature recuperator.

The mass of a low-temperature recuperator was estimated on the basis of its area and an assumed specific mass per unit area. The specific mass per unit area used herein is 3 kg/m^2. This would correspond to constructing the recuperator heat transfer surfaces with 15 mill steel. This specific mass per

unit area is consistent with that analyzed by Freedman[7].

The mass of the magnet plus MHD generator was assumed to be 0.45 kg/kWe (1 lb/kWe). This mass estimate appears to be reasonable based upon the technology of megawatt combustion generators and their superconducting magnets. The technology of the generator and magnet is discussed in more detail in a later section of this paper.

The mass of the turbine plus compressor is estimated on the basis of the total compressor power times a specific mass per unit compressor power. This specific mass is assumed to be 0.45 kg/kW (~3/4 lb/hp) of compressor power.

Total System Mass

With the above assumptions the total system masses of the turbo-MHD space power systems can be estimated if one assumes a low temperature recuperator specific area and the electric power output. However, the resulting masses of the recuperator and the radiator are respectively increasing and decreasing functions of the recuperator specific area. Thus, to evaluate the mass of the four turbo-MHD cycles fairly the specific area of the recuperator was chosen for each case so as to minimize the total mass of the recuperator plus radiator. The resulting parameters for the various cycles are tabulated in Table 4.

The total masses were then estimated for 10 MW_e space power systems using the four turbo-MHD cycles of Table 4. The component and total specific mass for the four cycles, each with the two shielding configurations, are listed in Table 5. The total specific masses of these power systems are all quite low. As indicated previously, they have relatively low radiator areas and high cycle efficiency. They are, thus, potentially very attractive space-power systems, and would lead to attractive electric rockets for future manned-planetary exploration or other high-payload missions.

Critical Component Technology

Reactor

To construct the reactor assumed in the analysis herein would be a significant technological achievement. The only reactors that have been operated to a temperature of 2500 K are those tested to establish the NERVA technology. These reactors have, of course, only demonstrated short time operation at these high exhaust gas temperatures. However, replacement of the highly active hydrogen coolant used in NERVA with an inert gas and reducing the power density two orders of magnitude (that required for the power applications herein) should result in greatly increased endurance capability.[1]

The NERVA reactors fuel element is constructed from many tiny pyro carbon coated UC_2 beads dispersed in a graphite matrix.[6] Although the existing NERVA fuel beads would probably not be adequate for the long-life high-temperature reactors envisioned herein, the potential of developing suitable advanced technology beads appears promising. The technology of such super beads is being investigated at General Atomics in conjunction with Los Alamos Scientific Laboratories. An alternative advanced

bead design is being investigated by Oak Ridge National Laboratory.

A schematic of a possible NERVA technology reactor configuration[6,12] for a power system is shown in Fig. 7. Although this reactor was designed for much lower reactor outlet temperatures (less than 1500 K) than is desired herein, it represents a general configuration and control technique that might be useable. For 2500 K applications, however, additional insulation and cooling may be required. Also, some of the low temperature materials in the design would need to be replaced.

Two major complications of using these graphite reactors for turbo-MHD power systems are the fission product release and the incompatibility of alkali metals with very high temperature graphite. Both these problems could be avoided if separately vented tungsten clad uranium dioxide or uranium nitride fuel elements could be used for the reactor. Such elements, however, have not demonstrated the high temperature capability desired for this application. Future technological improvements might make them useable for this application.

A promising technique for minimizing the preceding problems is to modify the turbo-MHD cycle by separating it into two loops. One such cycle is shown in Fig. 8. Physically, a heat exchanger has been inserted between the MHD generator loop and the turbine loop. The resulting two-loop cycle confines the fission product to the MHD generator loop which contains only one rotating piece of equipment, a compressor. This cycle also permits alkali seed to be injected into the working fluid between the reactor and the MHD generator and allows it to be condensed in the cooler preceeding the compressor. As a result, neither the reactor nor the compressor is required to operate with an alkali-seeded working fluid. The practicality of condensing cesium seed from the working fluid at the heat rejection temperature of a ground power station has already been demonstrated in the large German close-loop MHD generator experiment.[13] For space-power systems, the vapor pressure of cesium may be too high at the lowest temperature of the cycle, but condensing other alkali seeds such as lithium or possibly sodium should be practical. The performance of a turbo-MHD space-power system with these seeds would still be quite attractive and would be closer to the performance of the cesium system rather than the xenon system studied herein. One additional advantage of a two-loop turbo-MHD cycle is that the working fluids and pressures in the two loops could be separately optimized to achieve the maximum total system performance. The disadvantage of the two-loop system is that it requires an additional heat exchanger which would be similar in mass to the low-temperature recuperator.

MHD Generator

There are at present two large closed-loop alkali-seeded inert-gas MHD generator experiments in the world; one at the Lewis Research Center,[14,15] the other in Germany at Julich[13]. Russian plans to construct a third large closed loop experiment were recently announced. In addition, there are a number of blowdown, shock tube, and small arc heated experiments in both the U.S. and Europe[16] which are investigating inert-gas alkali-seeded MHD generators.

Both of the large closed loop MHD experiments are now producing some output power (approx. 100 W). A cut-away of the Lewis Research Center MHD generator facility is shown in Fig. 9. It makes use of a graphite resistance heater to heat 1.8 kg/sec of argon (preheated in the recuperator) to a temperature of 2000 K. The cesium seed is injected into the stream in the channel between the heater and the MHD duct. The MHD duct is segmented into 28 electrode pairs and the magnet provides a magnetic field of up to 2 T transverse to the stream. At present shorting paths between the conducting gas and the outer metallic duct skin prevent more than a small fraction of the power generated in the duct from being extracted through the electrodes. Duct design changes to eliminate this problem are being investigated. The German loop also appears to have shorting problems. In addition, their experiment is presently limited to operating temperatures below 1750 K and magnetic field strengths below 1 T.

One important feature of the German loop is their cesium seed recovery system. They are able to recover more than 99 percent of the seed in a condenser downstream of a recuperator and recycle the cesium into the seed injection system which is inside their tantalum resistance heater. Several experiments (the German loop experiment, blowdown experiments in Italy and the U.S., and shock tube driven experiments in both the U.S. and Russia) appear to indicate that a process known as nonequilibrium ionization can be achieved in an alkali-metal-seeded inert-gas MHD generator. This process results from the fact that the electrons are the preferential current carriers in a conducting gas. Since the electrons carry the current, they receive the resistive heating; thus, the electron temperature is elevated above the bulk gas temperature. Hence, the conductivity of the gas (which increases with electron temperature) tends to be higher than that appropriate to the gas temperature. The degree to which this process can be utilized is limited by the growth of plasma instabilities. Two necessary requirements for obtaining nonequilibrium elevation of the electron temperature in an MHD generator are (1) the MHD generator must be segmented in the stream-wise direction to prevent flow of any axial current, (2) the working fluid of the MHD generator must contain no major molecular impurities. In the Italian generator,[17] an increase of a factor of 10 above the equilibrium conductivity value has been achieved. Their nonequilibrium effects were limited by axial voltage breakdown between segments at electric fields of 38 V/cm.

The generator must be segmented because the flow of a conducting gas through a magnetic field induces both a transverse and an axial electric field. A generator can, however, be constructed so that for every cathode (electron emitter) there is at a station further downstream an anode (electron collector) that has the identical potential. These equal potential anodes and cathodes may be electrically connected together without affecting the generator performance. The total power output, the sum from all the electrode pairs, of such a diagonally connected generator is then extracted from a single upstream anode and downstream cathode. One simple method of constructing such a diagonally connected generator is to construct a circular duct from eliptical electrode segments separated by insulators. This is called a diagonal wall generator and offers the simplicity of construction and two terminal operation.

Using the best MHD generator theory which includes the effects of plasma instabilities and the resulting fluctuations, the size and shape of the MHD generators for the space power systems considered herein can be calculated by the procedure of Bishop and Nichols.[18] A 10 MW cesium seeded generator with an 80 percent efficiency having an input gas temperature of 2500 K at 10 atm and an inlet transverse magnetic field of 10 T would have a length of a half meter and an aspect ratio of three for a near sonic generator. (The aspect ratio is defined as the length divided by the square root of the entrance area.) To prevent aerodynamic choking in the generator, the generator area must increase slightly through the generator. To obtain a minimum volume generator at nearly constant power density, the area should increase slightly and the magnetic field should decrease slightly from the entrance to the exit of the generator.

A number of superconducting magnets have been constructed for combustion MHD generators. Figure 10 shows a magnet for a nominal 1 MW combustion generator. This magnet was constructed for the Air Force by the Airco Temescat Division of the Air Reduction Company. It has a design field of 7 T and has a 3/4 m length and can accept a 0.17 m diameter MHD duct. Its dewared weight is approximately 4000 lb, and it represents the state of the art a few years ago. Since its design, major strides have been made in the technology of such magnets. As a result, the magnets required for the 10 MW space power systems considered herein should have a weight under 10,000 lb, or close to 0.45 kg/kWe (1 lb/kWe).[19]

Concluding Remarks

Although technical feasibility questions regarding nuclear MHD systems remain, the advances in very high temperature gas cooled reactors and the encouraging results being obtained in closed-loop MHD generator experiments substantially increase the prospects for these systems. For space-power applications, these MHD systems would be attractive for electric propulsion. The resulting electric rockets, if mated with a nuclear rocket booster, would have a total mission time under a year for manned Mars landing missions. For terrestrial applications, these nuclear-MHD systems would be attractive for two types of systems. If cooling water is used as a heat sink, then the MHD systems high efficiency (approx. 60 percent) would lower by a factor of three the heat rejection per kWe of present nuclear power generators. Alternatively, a cycle efficiency of perhaps 45 percent could be obtainable with these MHD systems using only an air-cooled convector radiator as a heat sink. Such a power source would require no cooling water and might minimize the power plant's effect on the local ecology. By using a two-loop turbo-MHD cycle, the problems associated with fission product contamination of the stream and alkali-metal seeds can be minimized in these systems.

References

1. Holman, R. R. and Way, S., "Exploring a Closed Brayton Cycle MHD Power System Applying NERVA Reactor Technology," Paper 70-1225, Oct. 1970, AIAA, New York, N.Y.

2. Bohn, T. Komarek, P., and Noack, G., "Aspects of Essential Components of Nuclear MHD Plants," Eleventh Symposium on Engineering Aspects of

Magnetohydrodynamics, California Inst. Tech., Mar. 24-26, 1970, pp. 109-118.

3. Millionshchikov, M. D., Lynl'ka, A. U., Nedospasov, A. V., and Shendlin, A. E., "The Possibilities of Using Gas-Turbine Units and Magnetohydrodynamic Generators in Atomic Power Plants with High Temperature Gas Cooled Reactors," High Temperature, vol. 8, no. 2, Mar.-Apr. 1970, pp. 353-363.

4. Nichols, L. N., "A Combined Turbine-MHD Brayton Cycle for Space and Ground Use." Proposed NASA Technical Note.

5. Moeckel, W. E., "Propulsion Systems for Manned Exploration of the Solar System," TM X-1864, 1969, NASA, Cleveland, Ohio.

6. Anon., "The NERVA Technology Reactor Integrated with NASA Lewis Brayton Cycle Space Power System," WANL-TNR-225, May 1970, Westinghouse Electric Corp., Pittsburgh, Pa.

7. Freedman, S. I., "Study of Nuclear Brayton Cycle Power System," GE-65SD4251, NASA CR-54397, Aug. 1965, General Electric Co., Philadelphia, Pa.

8. Loewe, W. E., "Analysis of an Out-of-Core Thermionic Space Power System," IEEE Transactions on Aerospace and Electronic Systems, vol. AES-5, no. 1, Jan. 1969, pp. 58-65.

9. Zipkin, M. A., "Alkali-Metal, Rankine-Cycle Power Systems for Electric Propulsion," Journal of Spacecraft and Rockets, vol. 4, no. 7, July 1967, pp. 852-858.

10. Haller, H. C. and Lieblein, S., "Analytical Comparison of Rankine Cycle Space Radiators Constructed of Central, Double, and Block-Vapor-Chamber Fin-Tube Geometries," TN D-4411, 1968, NASA, Cleveland, Ohio.

11. Johnsen, R. L., "Weight Study of Partially Segmented Direct-Condensing Radiators for Large Space Power Systems," TN D-3227, 1966, NASA, Cleveland, Ohio.

12. Boman, L. H. and Gallagher, T. G., "NERVA Technology Reactor Integrated with NASA Lewis Brayton Cycle Space Power Systems," Paper 70-1226, Oct. 1970, AIAA, New York, N.Y.

13. Bohn, Th., Grawatsch, K., Holzapfel, Chr., Komarek, P., Lang, H., and Noack, G., "Measurements with ARGAS II," Closed Cycle Plasma MHD Systems. Vol. 2 of Fifth International Conference on Magnetohydrodynamic Electrical Power Generation, Munich, Apr. 19-23, 1971, vol. II, pp. 403-415.

14. Nichols, L. D., Morgan, J. L., Nagy, L. A., Lamberti, J. M., and Ellson, R. A., "Design and Preliminary Operation of the Lewis Magnetohydrodynamic Generator Facility," TN D-4867, 1968, NASA, Cleveland, Ohio.

15. Sovie, R. J. and Nichols, L. D., "Results Obtained in the NASA-Lewis Closed Cycle Magnetohydrodynamic Power Generation Experiments," TM X-2277, 1971, NASA, Cleveland, Ohio.

16. "Closed Cycle Power Generation Experiment," Section 2.6 of Closed Cycle Plasma MHD Systems. Vol. 2 of Fifth International Conference on Magnetohydrodynamic Electrical Power Generation, Munich, Apr. 19-23, 1971.

17. Gasparotto, M., Gay, P., Toschi, R., and Bertilini, E., "Constant Velocity Subsonic Experiments with Closed Cycle MHD Generator," Closed Cycle Plasma MHD Systems. Vol. 2 of Fifth International Conference on Magnetohydrodynamic Electrical Power Generation, Munich, Apr. 19-23, 1971, pp. 415-431.

18. Bishop, A. R. and Nichols, L. D., "Effect of Electrothermal Instabilities on Brayton- and Rankine-Cycle Magnetohydrodyanmic Space-Power Generation Systems," TN D-5461, 1969, NASA, Cleveland, Ohio.

19. Stekly, Z. J. J., Thome, R. J., and Cooper, R. F., "Characteristics of MHD Generator Systems Using Superconducting Field Coils," Fifth International Conference on Magnetohydrodynamic Electrical Power Generation, Munich, Apr. 19-23, 1971. (to be published in Vol. 4 of Proceedings).

TABLE 1. - ASSUMED CYCLE COMPONENT PERFORMANCE

Turbine efficiency, η_{TURB}	90%
Compressor efficiency, η_{COMP}	88%
High temperature recuperator heat loss	5%
Turbine reheater heat loss	5%
MHD generator efficiency, η_{GEN} Cesium seed Xeon seed	80% 55%

TABLE 2. - QUANTITIES USED TO EVALUATE SPECIFIC RECUPERATE PARAMETER, R

Cycle high pressure, P_H	10 atm
Recuperator friction factor, f	0.003
Ratio of specific heats, γ	5/3
Prandtl number, N_{PR}	0.714

TABLE 3. - CYCLE PARAMETERS FOR MINIMUM RADIATOR AREA SPACE POWER SYSTEMS. LOW TEMPERATURE RECUPERATOR SPECIFIC AREA, 0.374 m^2/kW_e.

Cycle	All MHD		Turbo-MHD				All Turbine	
Seed	Cs	Xe	Cs	Xe	Cs	Xe	----	----
Temperatures, K								
Reactor outlet	2500	2500	2500	2500	2500	2500	1500	1250
MHD exit	1567	1748	2070	2177	2148	2206	----	----
Turbine inlet	----	----	1500	1500	1250	1250	1500	1250
Radiator inlet	1144	890	883	874	739	730	713	591
Compressor: exit	1039	675	801	797	661	660	672	559
inlet	802	485	608	586	739	500	514	425
Cycle efficiency, %	21.4	18.7	38.4	30.2	40.4	32.9	22.5	22.6
Specific radiator area, m^2/kW_e	.0969	.659	.1202	.1898	.1987	.3184	.552	1.160
Ratio compressor to net electrical power	3.21	3.16	1.35	1.96	1.12	1.64	3.19	3.18
Fractional pressure drop, δ, %	4	6	0.6	1	0.6	1	6	6
Overall compression ratio	5	7.7	6.2	7.7	4.4	6.2	5	5.2

TABLE 4. - CYCLE PARAMETERS FOR TURBO-MHD SPACE-POWER SYSTEMS WITH MINIMUM RADIATOR PLUS LOW-TEMPERATURE RECUPERATOR MASS

Seed	Cs	Xe	Cs	Xe
Temperatures, K				
Reactor outlet	2500	2500	2500	2500
MHD exit	2019	2169	2071	2203
Reheater hot side exit	1678	1828	1817	1947
Turbines: inlet	1500	1500	1250	1250
exit	1176	1176	1008	1007
Radiator inlet	860	862	726	725
Compressors: inlet	564	564	494	493
exit	781	781	655	655
High-temperature recuperator cold side inlet	1097	1095	937	937
Reactor inlet	1266	1406	1476	1599
Cycle efficiency, %	38.9	30.3	41.9	33.0
Specific area, m^2/kW_e				
Radiator	.1465	.2136	.2280	.3333
Low temperature recuperator	.1726	.2517	.2111	.3026
Ratio compressor power to electric power	1.35	1.97	1.13	1.64
Overall compression ratio	8.33	8.33	6.37	6.45
Fractional pressure drop, δ, %	1.35	1.95	1.3	1.33

TABLE 5. - SPECIFIC MASS OF 2500 K, 10 MW TURBO-MHD SPACE-POWER SYSTEMS

Shield	10° Shadow				Shadow and Peripheral			
Turbine temperature, K	1500		1250		1500		1250	
Seed	Cs	Xe	Cs	Xe	Cs	Xe	Cs	Xe
Specific mass, kg/kW$_e$								
Reactor plus shield	0.61	0.73	0.57	0.68	1.93	2.15	1.87	2.07
Radiator	1.23	1.79	1.92	2.80	1.23	1.79	1.92	2.80
Low temperature recuperator	.52	.76	.63	.91	.52	.76	.63	.91
MHD generator and magnet	.45	.45	.45	.45	.45	.45	.45	.45
Turbines and compressors	.61	.89	.51	.74	.61	.89	.51	.74
Total	3.42	4.62	4.08	5.58	4.74	6.04	5.38	6.97

Figure 1. - Turbo-MHD cycle.

(A) VARIATION WITH MHD GENERATOR EFFICIENCY, η_{GEN}.

(B) VARIATION WITH LOW TEMPERATURE RECUPERATOR EFFECTIVENESS, η_r.

(C) VARIATION WITH OVERALL CYCLE COMPRESSION RATIO, r.

(D) VARIATION WITH FRACTIONAL PRESSURE DROP, δ.

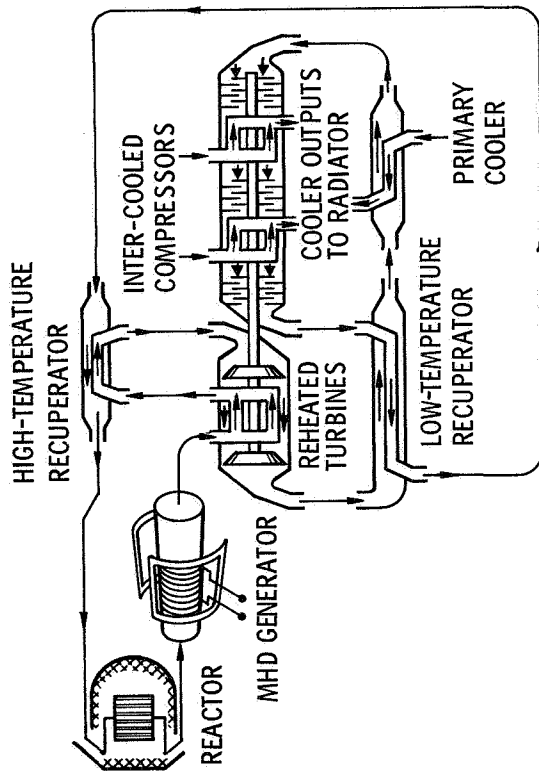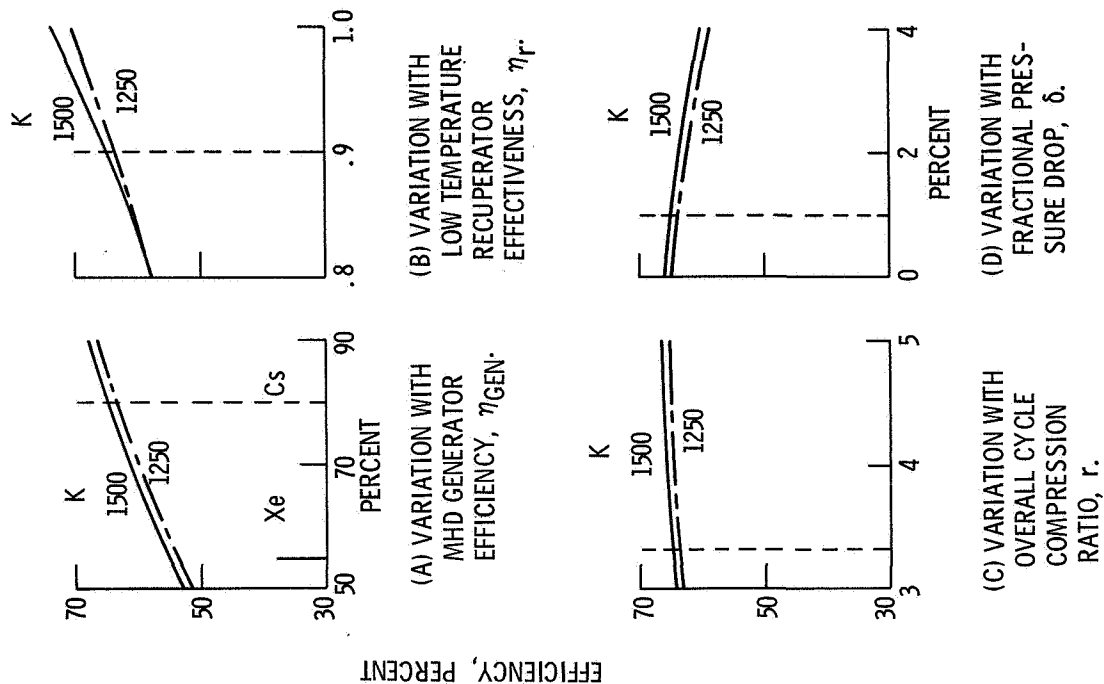EFFICIENCY, PERCENT

Figure 3. – Parametric variation of overall cycle efficiency of a 2500 K turbo-MHD ground-power station. Dashed lines indicates common conditions: η_{GEN} = 80 percent, η_r = 0.9, r = 3.33, δ = 1 percent; temperatures are turbine inlet
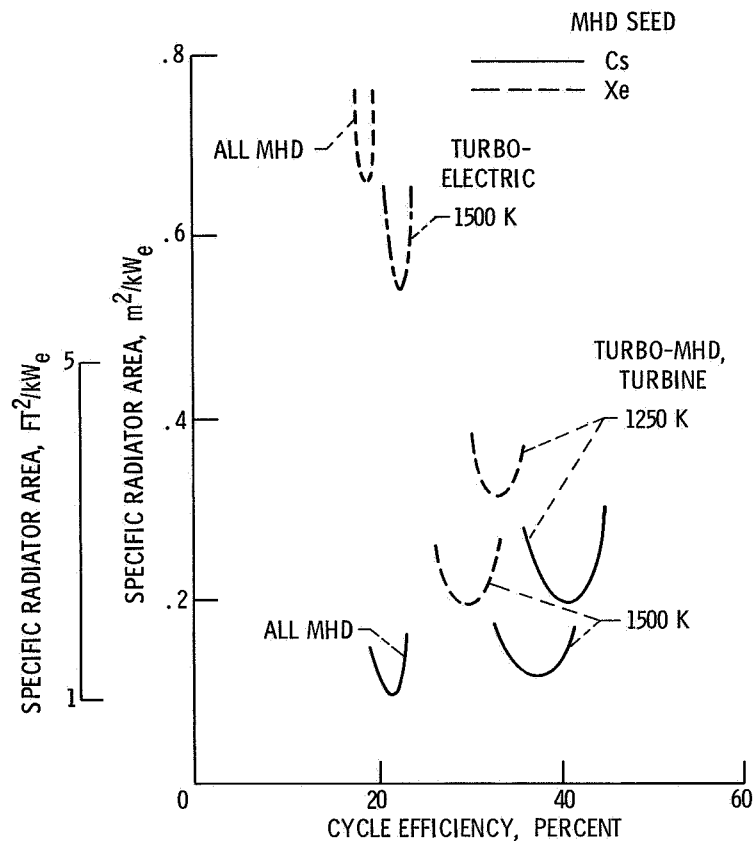

Figure 2. – Turbo-MHD power system.

Figure 4. - Specific radiator area as a function of space power system cycle efficiency.

(A) 10° SHADOW SHIELD.   (B) SHADOW + PERIPHERAL SHIELD.
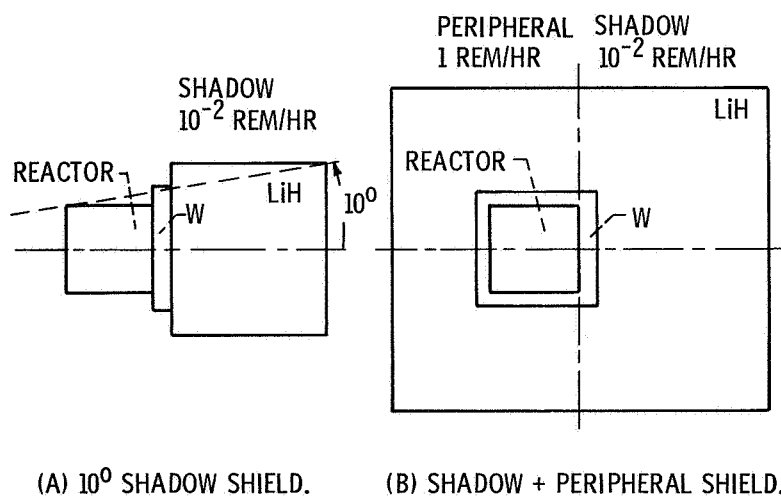
Figure 5. - Reactor and shield configurations.

E-6304

CORE SUPPORT
PLATE

Be REFLECTOR

GRAPHITE BARREL
AND LATERAL
SUPPORT SYSTEM

PRESSURE
VESSEL

ELECTRIC
ACTUATOR

Pb SHIELD

CONTROL
DRUM

CORE

SUPPORT
RING
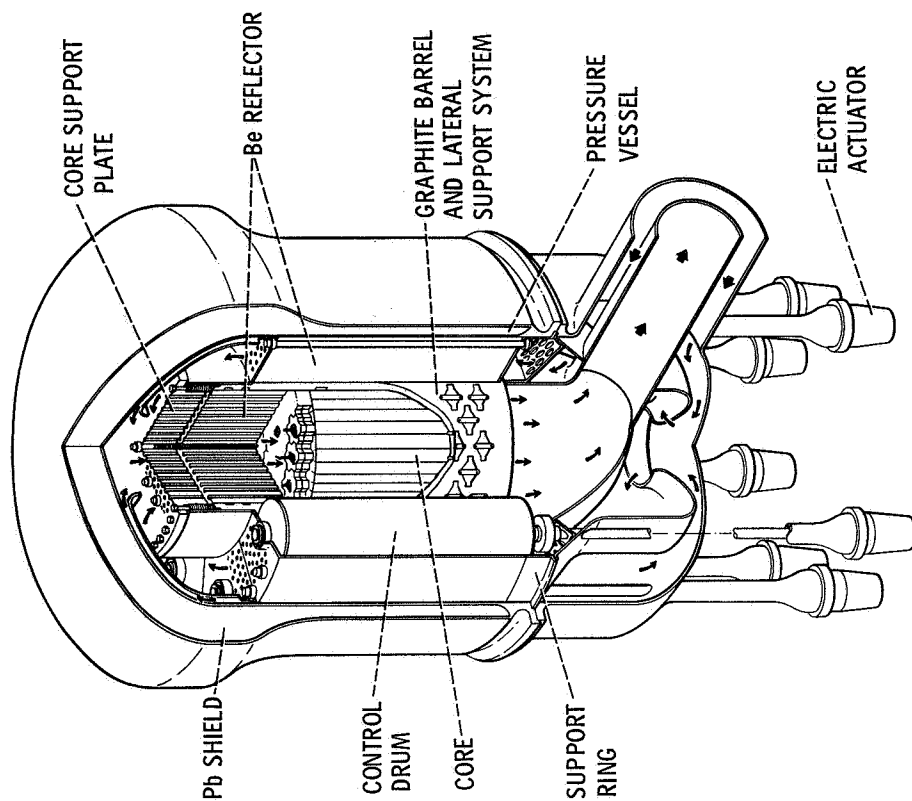
Figure 7. – NERVA technology reactor for Brayton cycle space power system. 6, 12

TYPE REACTOR

GAS COOLED
■   REF. 6
◆   REF. 7

OUT-OF-CORE THERMIONIC
○   REF. 8

RANKINE
▽   REF. 9

SHADOW + PERIPHERAL
SHIELD

10^0 SHADOW SHIELD
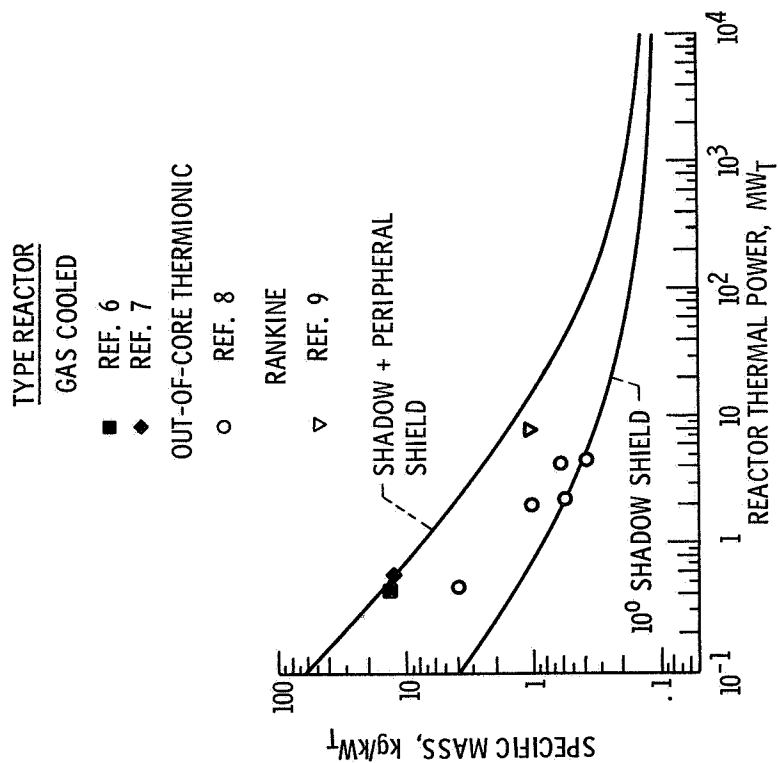
Figure 6. – Specific mass of reactor plus shield.
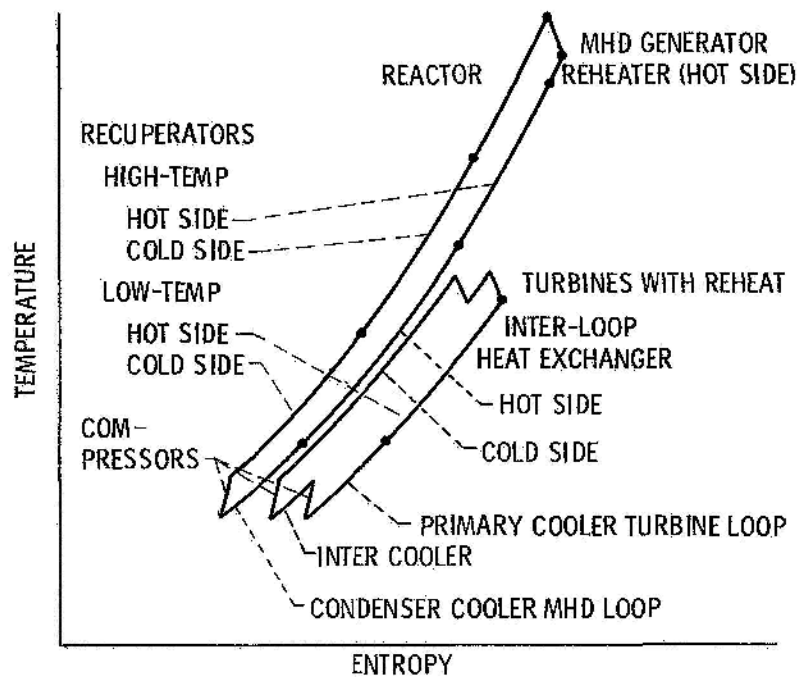
Figure 8. - Two-loop turbo-MHD cycle.

REACTOR

MHD GENERATOR
REHEATER (HOT SIDE)

RECUPERATORS
HIGH-TEMP
HOT SIDE
COLD SIDE
LOW-TEMP
HOT SIDE
COLD SIDE
COM-
PRESSORS

TURBINES WITH REHEAT
INTER-LOOP
HEAT EXCHANGER
HOT SIDE
COLD SIDE
PRIMARY COOLER TURBINE LOOP
INTER COOLER
CONDENSER COOLER MHD LOOP

TEMPERATURE

ENTROPY
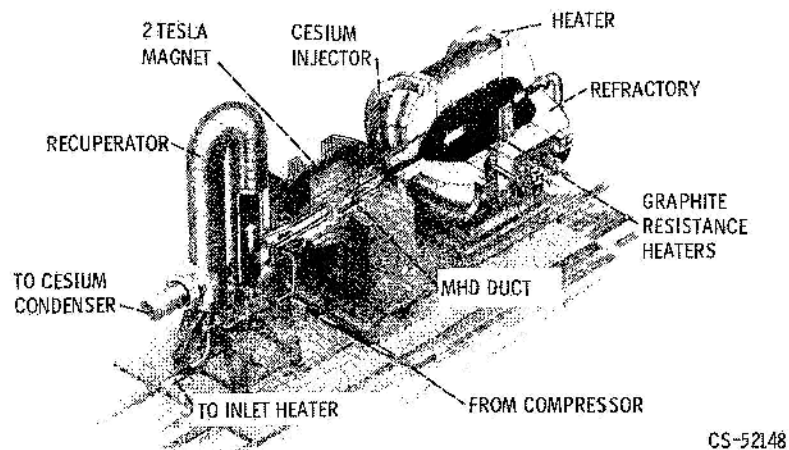
Figure 9. - Lewis Research Center MHD generator experiment.

2 TESLA
MAGNET

CESIUM
INJECTOR

HEATER

RECUPERATOR

REFRACTORY

TO CESIUM
CONDENSER

GRAPHITE
RESISTANCE
HEATERS
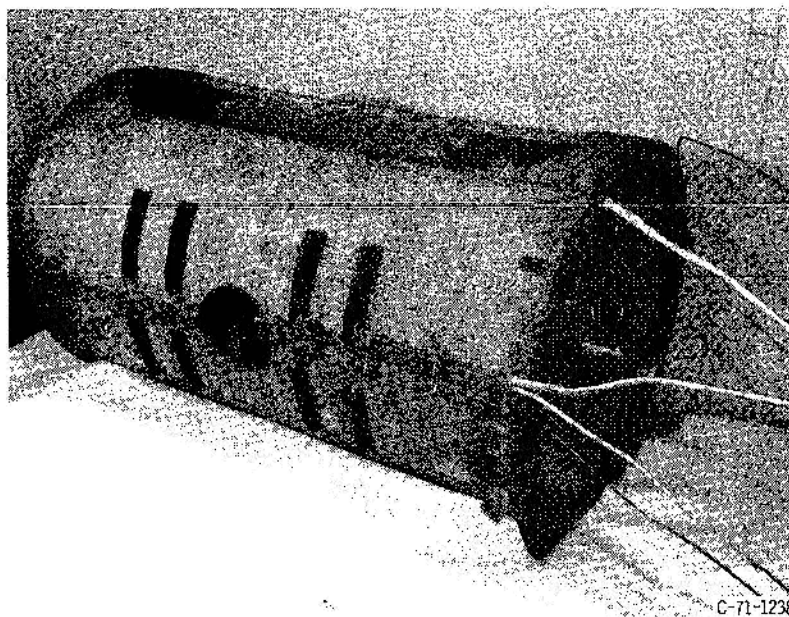
MHD DUCT

TO INLET HEATER

FROM COMPRESSOR

CS-52148

Figure 10. - Superconducting magnet for a MW MHD generator.